

Electro-osmotic flow near a surface charge discontinuity

By EHUD YARIV

Faculty of Mechanical Engineering, Technion – Israel Institute of Technology, Haifa 32000, Israel

(Received 2 April 2004 and in revised form 10 September 2004)

Electro-osmotic flows in the vicinity of surface charge density transitions are studied using a two-dimensional model problem. The analysed configuration consists of an electrolyte solution in contact with a dielectric planar wall, on which the density transition is approximated by a finite jump. The flow field in the semi-infinite fluid domain is driven by an external electric field which is applied parallel to the charged wall, in the direction of the jump. The problem is analysed using both the thin-Debye-layer (TDL) formulation, which does not resolve the fine details of the Debye-layer structure, and an approximate electrokinetic model.

1. Introduction

Many colloidal systems, both in nature and in engineering, are characterized by heterogeneous surface properties. For example, the walls of microfluidic channels may possess non-uniform charge distributions, resulting from imperfect fabrication processes or adsorption of charged analytes during electro-osmotic flow (Ghosal 2003). There is an increasing interest in flows associated with non-uniform surface charge profiles (Anderson & Idol 1985; Fair & Anderson 1989; Solomentsev, Pawar & Anderson 1993). Obviously, these flows exhibit richer physical phenomena (Anderson 1985; Long & Ajdari 1998) compared with those engendered by homogeneous surfaces.

Non-uniform surface charge is actually desirable in certain applications. The use of charge modulation was proposed by Ajdari (1995, 1996) as a means for generating complex electro-mechanical flows. Following Ajdari's work, it was soon realized that simple configurations possessing spatially periodic charge density profiles could operate as passive mixers in microfluidic devices. Such mixers are typically modelled using a two-dimensional geometry consisting of an infinite fluid strip bounded by two parallel planes, on which the charge distribution varies periodically.

While the initial studies of Ajdari considered the effects of sinusoidal charge distribution (which is relatively easy to analyse), later analyses focused on the more realistic case of piecewise continuous surface charge modulation, typically alternating between uniform values (Potoček *et al.* 1995; Stroock *et al.* 2000). The latter charge density configurations were modelled using the thin-Debye-layer (TDL) approximation, in which the details of the Debye layer are embodied in the Smoluchowski slip condition. In these TDL models the discontinuous density profiles are modelled by comparable discontinuous zeta potential distributions.

The linear TDL approximation, which has become a *de facto* standard in the engineering-oriented electrokinetic literature, constitutes a simple alternative to the fine-scale electrokinetic equation set (Saville 1977), which, being coupled and nonlinear, is challenging to handle. Note, however, that the underlying assumption of

the TDL model, namely a Debye-layer thickness that is small compared with all other length scales appearing in the problem, is not *a priori* guaranteed in the presence of surface charge discontinuities (of the kind appearing in the preceding references). Formally speaking, a charge density discontinuity represents a sharp transition region over a vanishingly small distance.

The purpose of this short paper is to provide, via a simple two-dimensional model, an initiatory description of the flow in the vicinity of a sharp transition between two uniform charge distributions. In a sense, this work constitutes the opposite extreme of lubrication models which describe slowly varying surface charge distributions (Long, Stone & Ajdari 1999; Ghosal 2002). The model problem selected consists of an infinite dielectric plane (positioned, say, at $\bar{y} = 0$), which is in contact with a semi-infinite fluid domain (viscosity μ , dielectric permittivity ϵ) filling the upper half-plane $\bar{y} > 0$. (In what follows, dimensional variables are denoted with overbars.) The plane possesses a discontinuous charge density $\bar{\sigma}(\bar{x})$, say $\bar{\sigma}_<$ for $\bar{x} < 0$ and $\bar{\sigma}_>$ for $\bar{x} > 0$. An external electric field E is applied in the positive \bar{x} -direction. Our goal is to describe the resulting flow field using both the TDL model and an approximate electrokinetic model.

2. Thin-Debye-layer approximation

The TDL approximation is appropriate if the Debye-layer thickness λ (see (3.1)) is small compared with the characteristic linear dimension of the problem. This scale disparity naturally leads to a singular description (Keh & Anderson 1985), wherein the layer is taken to be infinitely thin. The electric potential in the neutral ‘bulk’ fluid domain is therefore governed by Laplace’s equation, and the flow field is described by the standard Stokes equation, without any electrical body forces. The presence of free charge in the TDL is nevertheless implicit in the boundary conditions applicable at the boundaries of the bulk, namely the homogeneous no-flux requirement,

$$\hat{n} \cdot \bar{\nabla} \bar{\phi} = 0, \quad (2.1)$$

governing the electric potential $\bar{\phi}$ (with \hat{n} a unit vector normal to the boundary), and the Helmholtz–Smoluchowski equation,

$$\bar{v} = \frac{\epsilon \bar{\zeta}}{\mu} \bar{\nabla} \bar{\phi}, \quad (2.2)$$

governing the ‘slip’ value of the velocity field \bar{v} relative to the charged wall. The zeta potential $\bar{\zeta}$ constitutes the excess electric potential (relative to the respective bulk value) at the surface, and is a function of the local charge density. The linear conditions (2.1)–(2.2) neatly merge with Laplace’s and Stokes’ equations, which control the electrostatics and flow in the electrically neutral bulk domain.

In the present two-dimensional fluid–wall configuration, it is obvious that the electric potential corresponding to the externally applied field, $\bar{\phi} = -E\bar{x}$, trivially satisfies the impermeability condition (2.1) at $\bar{y} = 0$ and is therefore valid throughout the fluid domain. Thus, the TDL analysis amounts to the calculation of the velocity field, $\bar{v} = \bar{u}\hat{x} + \bar{v}\hat{y}$, which is governed by the Stokes equations together with the slip and no-flux conditions,

$$\begin{cases} \bar{u} = -\epsilon \bar{\zeta}(\bar{x})E/\mu, \\ \bar{v} = 0, \end{cases} \quad \text{at} \quad \bar{y} = 0. \quad (2.3)$$

Within the present TDL framework, the charge distribution discontinuity is modelled by a comparable discontinuity in the zeta potential $\bar{\zeta}(\bar{x})$, namely $\bar{\zeta} = \bar{\zeta}_<$ for $\bar{x} < 0$ and $\bar{\zeta} = \bar{\zeta}_>$ for $\bar{x} > 0$ (cf. Stroock *et al.* 2000).

It is convenient to decompose the flow problem into a symmetric problem, corresponding to a uniform zeta potential, $\bar{\zeta}_S = (\bar{\zeta}_> + \bar{\zeta}_<)/2$, and an antisymmetric problem, where $\bar{\zeta} = \bar{\zeta}_A \stackrel{\text{def}}{=} (\bar{\zeta}_> - \bar{\zeta}_<)/2$ for $\bar{x} > 0$ and $\bar{\zeta} = -\bar{\zeta}_A$ for $\bar{x} < 0$.

The solution to the symmetric problem is the trivial plug flow,

$$\bar{v}_S = -\hat{x} \frac{\epsilon \bar{\zeta}_S E}{\mu}. \quad (2.4)$$

To calculate the velocity field of the antisymmetric problem, $\bar{v}_A = \bar{u}_A \hat{x} + \bar{v}_A \hat{y}$, it is convenient to employ the stream function, $\bar{\psi}_A$, defined by the kinematic relations

$$\bar{u}_A = -\frac{\partial \bar{\psi}_A}{\partial \bar{y}}, \quad \bar{v}_A = \frac{\partial \bar{\psi}_A}{\partial \bar{x}}. \quad (2.5)$$

This function satisfies the bi-harmonic equation

$$\bar{\nabla}^4 \bar{\psi}_A = 0, \quad (2.6)$$

and the boundary conditions at the solid wall, $\bar{y} = 0$,

$$\frac{\partial \bar{\psi}_A}{\partial \bar{x}} = 0, \quad \frac{\partial \bar{\psi}_A}{\partial \bar{y}} = \begin{cases} U & \text{at } \bar{x} > 0, \\ -U & \text{at } \bar{x} < 0, \end{cases} \quad (2.7)$$

where $U = \epsilon \bar{\zeta}_A E / \mu$.

The model problem considered does not possess any length scale with which the coordinates \bar{x} and \bar{y} can be normalized. Thus, dimensional considerations require that the scaled stream function $\bar{\psi}_A/U$ (which has the dimensions of length) possesses the similarity form $\bar{\psi}_A/U = \bar{r}F(\theta)$, wherein \bar{r} and θ respectively denote the radial and azimuthal coordinates in a polar representation. Use of the general solution of two-dimensional Stokes flows (Leal 1992) readily yields

$$\frac{\bar{\psi}_A}{U} = \frac{2\bar{r}}{\pi} \left(\frac{\pi}{2} - \theta \right) \sin \theta \left[= \frac{2\bar{y}}{\pi} \arctan \frac{\bar{x}}{\bar{y}} \right]. \quad (2.8)$$

Note that for $\bar{x}/\bar{y} \rightarrow \pm\infty$ the velocity field (normalized with U) approaches the expected plug values $\mp \hat{x}$.

3. Electrokinetic analysis

The velocity field (2.8) implies velocity gradients that vary as $1/\bar{r}$, and, consequently, viscous stresses that diverge near the origin. This was to be expected, given the discontinuity in the jump condition along the plane $\bar{y} = 0$. This singularity, of course, is only an artifact of the TDL approximation: in the Debye-layer scale the fluid adheres to the wall and no flow discontinuity is realized.

To resolve this singularity, we analyse here the charge-discontinuity problem using a fine-scale electrokinetic description, which – unlike its TDL counterpart – unfolds the details of the Debye cloud. For simplicity, we focus upon the case of a symmetric $z-z$ solution, where both the co- and counter-ions possess identical valence z and equilibrium concentration n_∞ . In non-dimensionalizing the various variables, we select

the Debye-layer thickness

$$\lambda = \left(\frac{\epsilon kT}{2z^2 e^2 n_\infty} \right)^{1/2} \quad (3.1)$$

as the length unit. The balance between migration and diffusion yields the electric potential scale $\phi_0 = kT/e$. The electric body force introduces the stress scale $T_0 = \epsilon \phi_0^2 / \lambda^2$, which, when balanced against viscous stresses, provides the velocity scale $U_0 = T_0 \lambda / \mu$. The electric field is normalized with ϕ_0 / λ . In what follows, dimensionless variables appear without overbars.

The externally applied field is given by $\beta \hat{x}$, where $\beta = \lambda E / \phi_0$. Even for the strong fields encountered in microfluidic devices, say $E \sim 10000 \text{ V m}^{-1}$, the value of β is small owing to the small values of λ . Indeed, for λ on the order of nanometers one obtains $\beta \sim 10^{-4}$, and even for relatively thick Debye layers, say $0.1 \mu\text{m}$, $\beta \sim 0.01$. We therefore analyse first the equilibrium Debye structure, in the absence of an applied field. The electro-osmotic flow is later obtained as a small perturbation.

3.1. Equilibrium Debye-layer structure

As is common in the literature (see e.g. Ajdari 1995), we employ here the low-zeta-potential electrokinetic model. Thus, the equilibrium Debye cloud is governed by the linearized Boltzmann–Poisson (LBP) equation,

$$\nabla^2 \phi = \phi. \quad (3.2)$$

This equation is to be solved subject to the boundary condition at $y=0$,

$$\hat{y} \cdot \nabla \phi = -\sigma, \quad (3.3)$$

expressing the presence of charge on the dielectric wall, and the far-field condition away from the wall,

$$\nabla \phi \rightarrow \mathbf{0}, \quad (3.4)$$

reflecting the absence of an applied electric field. Here, $\sigma = (\lambda / \epsilon \phi_0) \bar{\sigma}$ is a dimensionless surface charge concentration, $\sigma = \sigma_>$ for $x > 0$ and $\sigma = \sigma_<$ for $x < 0$.

As with the TDL analysis, it is convenient to decompose the linear problem governing ϕ into a symmetric problem, corresponding to a uniform charge density $\sigma_S = (\sigma_> + \sigma_<) / 2$, and an antisymmetric problem, where the charge density is given by $\sigma_A = (\sigma_> - \sigma_<) / 2$ for $x > 0$ and by $-\sigma_A$ for $x < 0$. Accordingly, the electric potential is decomposed via the representation

$$\phi = \sigma_S \phi_S + \sigma_A \phi_A, \quad (3.5)$$

in which ϕ_S and ϕ_A respectively satisfy the following boundary conditions at $y=0$:

$$\frac{\partial \phi_S}{\partial y} = -1, \quad \frac{\partial \phi_A}{\partial y} = -\text{sgn}(x), \quad (3.6)$$

as well as the LBP equation (3.2) and the far-field attenuation condition (3.4).

It is readily verified that the symmetric part of the electric potential possesses the familiar one-dimensional solution

$$\phi_S = e^{-y}, \quad (3.7)$$

and it is again the antisymmetric problem which poses the difficulty. This problem is solved by applying the Fourier Sine transform,

$$\mathcal{F} \{f(x)\} = \int_{-\infty}^{\infty} f(x) \sin kx \, dx, \quad (3.8)$$

to the LBP equation and the boundary conditions governing ϕ_A . The Sine transform of the sign function exists in the generalized sense, and is given by $k/(k^2 + \delta^2)$, where δ is a positive number approaching zero. Requiring a solution that attenuates at large values of y provides the following expression for $\Phi_A(k, y) = \mathcal{F}\{\phi_A(x, y)\}$:

$$\Phi_A(k, y) = \frac{k \exp(-\sqrt{1+k^2}y)}{(k^2 + \delta^2)\sqrt{1+k^2}}. \tag{3.9}$$

Thus, the electric potential is given by the inverse transform

$$\phi_A(x, y) = \frac{2}{\pi} \int_0^\infty \frac{dk}{k\sqrt{1+k^2}} \exp(-y\sqrt{1+k^2}) \sin kx. \tag{3.10}$$

(In this expression δ is set to zero, since the singularity at $k=0$ is a removable one.) For large values of x the major contribution to (3.10) originates from the region $k \sim O(x^{-1})$. Use of the scaled integration variable $u = kx$ readily yields $\phi_A \sim \text{sgn}(x) e^{-y}$. Thus, the total electric potential (3.5), consisting of the symmetric (3.7) and anti-symmetric (3.10) distributions, behaves as $\sigma_> e^{-y}$ for $x \rightarrow \infty$, and as $\sigma_< e^{-y}$ for $x \rightarrow -\infty$ (as would have been expected). In accordance with the definition of the zeta potential, $\sigma_>$ and $\sigma_<$ are respectively identified with $\bar{\zeta}_>/\phi_0$ and $\bar{\zeta}_</\phi_0$.

To obtain an alternative expression for ϕ_A we represent it as an exponential Fourier transform (in this case δ cannot be set to zero). Since ϕ_A is an odd function of x we can consider only the case $x > 0$. The integral appearing in the transform is evaluated on a closed path in the complex k -plane, consisting of the real axis, two circular arcs C_1 and C_2 enclosing the upper half-plane, and the path C_3 encircling the branch cut which originates at $k=i$. As the radii of the semicircular arcs become large, the contribution from $C_1 \cup C_2$ becomes exponentially small. Use of the residue theorem furnishes the following expression:

$$\phi_A(x, y) = e^{-y} - \frac{1}{i\pi} \int_{C_3} \frac{k \exp(ikx - \sqrt{1+k^2}y)}{\sqrt{1+k^2}(k^2 + \delta^2)} dk, \tag{3.11}$$

the first term of which originates from the residue of the simple pole at $i\delta$. When performing the integration along the branch cut, δ may be set to zero. Evaluation and simplification of the resulting integral eventually provides the expression

$$\phi_A(x, y) = e^{-y} - \frac{2}{\pi} \int_0^\infty \frac{dt}{1+t^2} \exp(-\sqrt{1+t^2}x) \cos ty, \tag{3.12}$$

which is more convenient for numerical evaluation.

The first term in (3.12) is the expected electric field distribution far from the transition at $x=0$. To obtain the leading-order correction for $x \gg 1$ and $y \sim O(1)$ we note that the major contribution to the second term comes from the region near $t=0$; use of the scaled integration variable $u = x(\sqrt{1+t^2} - 1)$ readily furnishes the refined expression

$$\phi_A \sim e^{-y} - \sqrt{\frac{2}{\pi x}} e^{-x} \quad \text{for} \quad x \gg 1. \tag{3.13}$$

It is also interesting to obtain the behaviour of ϕ_A near the transition at $x=0$. Here, a straightforward asymptotic evaluation of the integral appearing in (3.10) yields

$$\phi_A \sim \frac{2x}{\pi} K_0(y) + o(x) \quad \text{for} \quad x \ll 1. \tag{3.14}$$

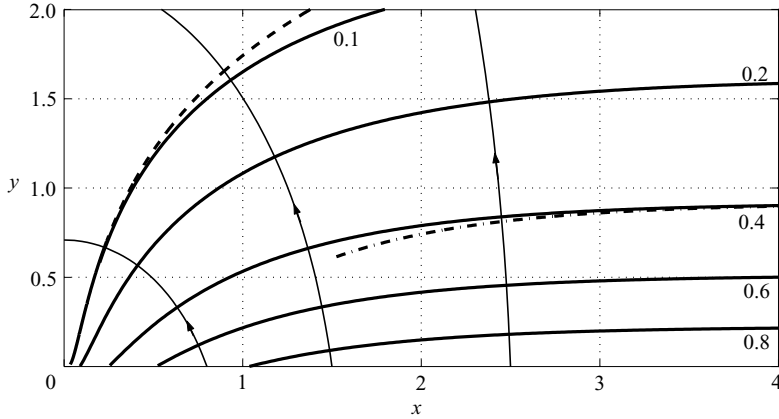


FIGURE 1. Equipotential lines, $\phi_A = \text{const}$, for the indicated values of ϕ_A (bold solid lines), obtained using (3.12). The line $\phi_A = 0.4$ is redrawn (dash-dotted line) using the large- x approximation (3.13) and the line $\phi_A = 0.1$ is redrawn (dashed line) using the small- x approximation (3.14). Several representative field lines are also presented (thinner solid lines).

As is to be expected from symmetry considerations, the predicted electric field at $x = 0$ is parallel to the wall, $-(2\sigma_A/\pi)K_0(y)\hat{x}$. The logarithmic singularity at small values of y results from the charge discontinuity at $y = 0$.

The equipotential lines $\phi_A = \text{const}$, obtained from (3.12), are depicted in figure 1. (Owing to the symmetry of the problem it is sufficient to confine the figure to the first quadrant in the xy -plane.) Within the scope of the linearized Boltzmann–Poisson approximation (3.2), these lines coincide with the contours of equal charge density: ϕ_A is therefore identical to the density value, normalized with $-\epsilon\phi_0/\lambda^2$. Note that the contour $\phi_A = 1$ coincides with the x -axis for large values of x , and that ϕ_A vanishes on the y -axis, as well as for large values of y .

3.2. Electro-osmotic flow

The non-equilibrium flow and transport processes occurring in the presence of an externally applied electric field are governed by a set of coupled equations, which are difficult to solve even for the simplest geometries. Our present goal, however, is not a rigorous solution for the exact electrokinetic problem, but rather an approximate description, which could be compared to the TDL results. Accordingly, we employ the model of Henry (1931), which assumes that the external field does not significantly distort the equilibrium Debye-layer structure. This model, which has been used to investigate electrophoretic retardation effects, is embodied in the approximate momentum balance,

$$\nabla p = \nabla^2 \mathbf{v} - \hat{x}\beta\nabla^2\phi, \tag{3.15}$$

in which the last term reflects the action of the external electric field, $\beta\hat{x}$, on the Debye-layer charge density, $-\nabla^2\phi$. (This is, of course, an exact equation in the case of a uniformly charged plane.)

As usual, the flow field is decomposed into symmetric and antisymmetric parts. It is convenient here to express \mathbf{v} as

$$\mathbf{v} = \beta(\sigma_S \mathbf{v}_S + \sigma_A \mathbf{v}_A) \tag{3.16}$$

and employ a similar representation for p . It is readily verified using (3.7) that the symmetric flow possesses the familiar unidirectional profile,

$$\mathbf{v}_S = (e^{-y} - 1)\hat{x}, \tag{3.17}$$

which, for large y , coincides with the plug flow described by the dimensionless counterpart of (2.4). Notice that the convergence is exponentially fast.

This equation governing the antisymmetric flow is written in the form

$$\nabla \times \zeta_A + \hat{x} \nabla^2 \phi_A + \nabla p_A = 0, \tag{3.18}$$

where $\zeta_A = \nabla \times \mathbf{v}_A$ is the anti-symmetric part of the vorticity field. Forming the curl of (3.18) and making use of (3.2) yields the simplified equation,

$$\nabla \times (\nabla \times \zeta_A) = \frac{\partial \phi_A}{\partial y} \hat{z},$$

which is independent of p_A . At this stage it is convenient to introduce the stream function ψ_A (normalized with λU_0):

$$u_A = -\frac{\partial \psi_A}{\partial y}, \quad v_A = \frac{\partial \psi_A}{\partial x}. \tag{3.19}$$

Noting that $\zeta_A = \hat{z} \nabla^2 \psi_A$, in which $\nabla^2 \psi$ is independent of z , we obtain a modified bi-harmonic equation (cf. (2.6)),

$$\nabla^4 \psi_A = -\frac{\partial \phi_A}{\partial y}, \tag{3.20}$$

which is to be solved subject to the impermeability and no-slip conditions on the charged wall (cf. (2.7)),

$$\frac{\partial \psi_A}{\partial x} = \frac{\partial \psi_A}{\partial y} = 0 \quad \text{at} \quad y = 0, \tag{3.21}$$

as well as the far-field condition, $\nabla p_A \rightarrow \mathbf{0}$ (or, equivalently, $\nabla^2 \mathbf{v}_A \rightarrow \mathbf{0}$).

Forming the Fourier Sine transform (3.8) of (3.20)–(3.21) yields the following equation governing $\Psi_A(k, y) = \mathcal{F}\{\psi_A(x, y)\}$:

$$\frac{d^4 \Psi_A}{dy^4} - 2k^2 \frac{d^2 \Psi_A}{dy^2} + k^4 \Psi_A = -\frac{d\Phi_A}{dy}.$$

This equation is to be solved subject to the boundary conditions at $y=0$, $\Psi_A = \partial \Psi_A / \partial y = 0$, as well as a far-field condition precluding divergence of Ψ_A at large values of y . Finding the required solution, and applying to it the inverse transform, $\psi_A(x, y) = (2/\pi) \int_{-\infty}^{\infty} dk \Psi_A(y; k) \sin kx$, eventually yields

$$\psi_A = \frac{2}{\pi} \left[y \int_0^{\infty} dk \frac{\sqrt{1+k^2}}{k} e^{-ky} \sin kx + \int_0^{\infty} dk \frac{e^{-y\sqrt{1+k^2}}}{k} \sin kx - \arctan \frac{x}{y} - \frac{xy}{x^2 + y^2} \right]. \tag{3.22}$$

The two integrals appearing in (3.22) do not seem to be expressible in closed form.

3.3. Comparison between models

Making use of the definition of β and the relation between $\bar{\zeta}$ and σ , we find that the dimensionless counterpart of the TDL prediction (2.8) is given by

$$\tilde{\psi}_A = \frac{2y}{\pi} \arctan \frac{x}{y}. \tag{3.23}$$

Comparing this expression with (3.22) requires the approximation of ψ_A for large r and fixed θ (that is, $y/x \sim O(1)$). In this limit, the second integral in (3.22) is

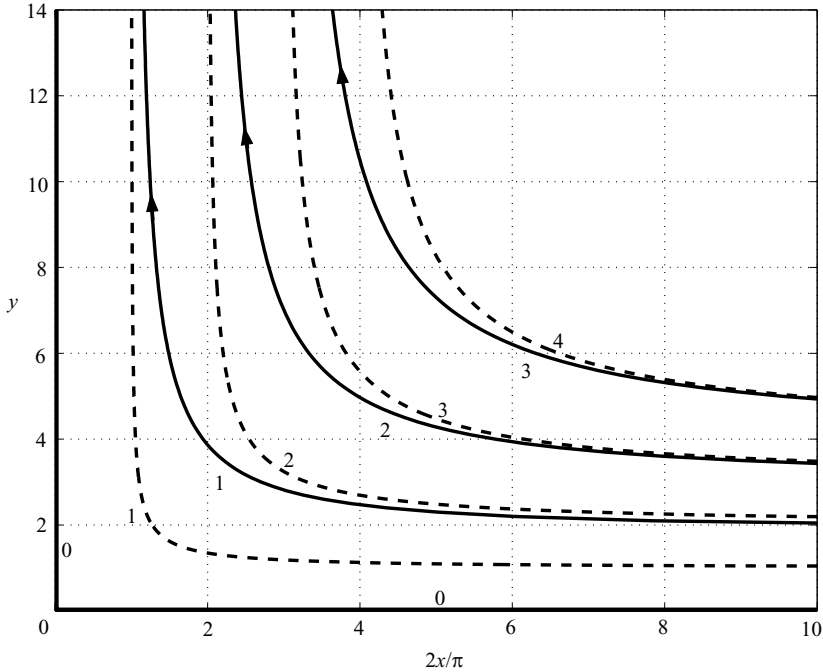


FIGURE 2. The streamlines $\psi_A = \text{const}$ (solid lines) and $\tilde{\psi}_A = \text{const}$ (dashed lines) for the indicated values of the stream functions. The arrows which signify the direction of the flow correspond to a positive value of σ_A .

exponentially small, and the main contribution to the first integral, which arises from the region near $k=0$, is obtained by use of the integration variable $u = kx$. This procedure yields

$$\psi_A \sim \frac{2}{\pi} \left[\left(\frac{\pi}{2} - \theta \right) r \sin \theta - \left(\frac{\pi}{2} - \theta \right) - \sin \theta \cos \theta + O(r^{-1}) \right] \quad \text{as } r \rightarrow \infty. \quad (3.24)$$

As expected, the $O(r)$ leading term in (3.24) coincides with $\tilde{\psi}_A$. However, the TDL approximation differs with (3.24) by an $O(1)$ term. In terms of the velocity field, this mismatch results in a slow algebraic approach (on the Debye scale) of the TDL approximation to the true velocity field. This contrasts with the exponentially decaying error existing in a uniform (or slowly varying) surface charge (Keh & Anderson 1985).

When considering the different limit of large x and fixed y , the second integral in (3.22) is not negligible, but rather admits a finite contribution from the region near $k=0$. Asymptotic evaluation of the two integrals yields

$$\psi_A \sim e^{-y} - 1 + y \quad \text{as } x \rightarrow \infty. \quad (3.25)$$

This expression corresponds to the velocity profile $u_A = e^{-y} - 1$, which is the expected low-zeta-potential distribution in a Debye layer adjacent to a surface of unity areal charge. Note that the TDL expression (2.8) degenerates to a different expression in the limit $x \rightarrow \infty$, namely $\tilde{\psi}_A \sim y$. The unity difference for $y \gg 1$ represents the Debye-layer flux which is unaccounted for in the TDL model.

The streamlines $\psi_A = \text{const}$ and $\tilde{\psi}_A = \text{const}$, respectively depicted using (3.22) and (3.23), are presented in figure 2. The $O(1)$ mismatch between the two models is clearly

noticeable. For large values of γ the streamline $\tilde{\psi}_A = C$ approaches the asymptote $x = \pi C/2$, in agreement with (3.23).

3.4. Concluding remarks

The principal outcomes of this paper are the antisymmetric TDL and LBP approximations to the velocity field in the neighbourhood of the charge discontinuity – both of $O(\epsilon \tilde{\zeta}_A E/\mu)$. Whereas the similarity TDL solution becomes discontinuous near the origin, the fine-scale LBP expression avoids this singularity owing to the presence of the length scale λ with which the spatial coordinates can be normalized.

The applicability of the present analysis to processes occurring in real devices is limited by the underlying idealized formulation, which reflects the desire for the simplest model possible. Thus, the assumption of charge discontinuity at the λ -scale constitutes a reasonable approximation only for dilute solutions, see (3.1), whereas the TDL similarity solution becomes invalid at the scale of the device itself. Nevertheless, the qualitative indications of the present model may guide future models of miniaturized flow systems, which would bridge the gap between the Debye-scale details of the wall charge distribution on one hand, and the device-scale geometry on the other.

The author thanks Professor Anthony M. J. Davis for many useful suggestions.

REFERENCES

- AJDARI, A. 1995 Electroosmosis on inhomogeneously charged surfaces. *Phys. Rev. Lett.* **75**, 755–758.
- AJDARI, A. 1996 Generation of transverse fluid currents and forces by an electric field: Electroosmosis on charge-modulated and undulated surfaces. *Phys. Rev. E* **53**, 4996–5005.
- ANDERSON, J. L. 1985 Effect of nonuniform zeta potential on particle movement in electric fields. *J. Colloid Interface Sci.* **105**, 45–54.
- ANDERSON, J. L. & IDOL, W. K. 1985 Electroosmosis through pores with nonuniformly charged walls. *Chem. Engng Commun.* **38**, 93–106.
- FAIR, M. C. & ANDERSON, J. L. 1989 Electrophoresis of nonuniformly charged ellipsoidal particles. *J. Colloid Interface Sci.* **127**, 388–400.
- GHOSAL, S. 2002 Lubrication theory for electro-osmotic flow in a microfluidic channel of slowly varying cross-section and wall charge. *J. Fluid Mech.* **459**, 103–128.
- GHOSAL, S. 2003 The effect of wall interactions in capillary-zone electrophoresis. *J. Fluid Mech.* **491**, 285–300.
- HENRY, D. C. 1931 The cataphoresis of suspended particles. Part I. The equation of cataphoresis. *Proc. R. Soc. Lond. A* **133**, 106–129.
- KEH, H. J. & ANDERSON, J. L. 1985 Boundary effects on electrophoretic motion of colloidal spheres. *J. Fluid Mech.* **153**, 417–439.
- LEAL, L. G. 1992 *Laminar Flow and Convective Transport Processes*. Butterworths-Heinemann.
- LONG, D. & AJDARI, A. 1998 Symmetry properties of the electrophoretic motion of patterned colloidal particles. *Phys. Rev. Lett.* **81**, 1529–1532.
- LONG, D., STONE, H. A. & AJDARI, A. 1999 Electroosmotic flows created by surface defects in capillary electrophoresis. *J. Colloid Interface Sci.* **212**, 338–349.
- POTOČEK, B., GAŠ, B., KENNDLER, E. & ŠTĚDRÝ, M. 1995 Electroosmosis in capillary zone electrophoresis with nonuniform zeta-potential. *J. Chromatography A* **709**, 51–62.
- SAVILLE, D. A. 1977 Electrokinetic effects with small particles. *Annu. Rev. Fluid Mech.* **9**, 321–337.
- SOLOMENTSEV, Y. E., PAWAR, Y. & ANDERSON, J. L. 1993 Electrophoretic mobility of nonuniformly charged spherical-particles with polarization of the double-layer. *J. Colloid Interface Sci.* **158**, 1–9.
- STROOCK, A. D., WECK, M., CHIU, D. T., HUCK, W. T. S., KENIS, P. J. A., ISMAGILOV, R. F. & WHITESIDES, G. M. 2000 Patterning electro-osmotic flow with patterned surface charge. *Phys. Rev. Lett.* **84**, 3314–3317.